Journal of Himalayan Earth Sciences Volume 58, No. 2, 2025 pp. 162-187

Tectonostratigraphic Evolution of the Kalat and Mach area, Northern Kirthar Range, Balochistan Basin, Pakistan

Mohammad Irfan Khan*[1, 3], Sajjad Ahmad[1], Sajjad Ahmad[2], Gohar Rehman[1], Salik Javed[3], Benazeer Iqbal[3], and Irfan Faiz[1]

[1] Department of Geology, University of Peshawar, 25120, Peshawar, Pakistan
[2] Geological Survey of Pakistan, Sariab Road, Quetta, Pakistan
[3] DeGolyer & MacNaughton Corporate, 5001 Spring Valley Road., Suite 800 East, Dallas, Texas
[*]Corresponding Author: irfan.uop.ik@gmail.com
Submitted Date: 04/02/2025 Acceptance Date: 12/05/2025 Publication Date: 30/11/2025

Abstract

In this study, the stratigraphic and sedimentological data have been utilized to decipher the tectonostratigraphic evolution of the Kalat and Mach area of the northern Kirthar Range, Balochistan Basin, Pakistan. Three (3) stratigraphic sections are measured, and the Jurassic-Paleogene facies variation with their depositional environments is documented in the study area. Based on the biostratigraphic and facies augmented information, four tectonostratigraphic evolution stages are described which include a) The late early Jurassic (Toarcian)-mid Jurassic (Callovian-Aalenian) around 180 Ma-159.4 Ma; the deposition of Anjira-Chiltan Formation, and a late Jurassic thermal uplift; preceding the Indo-Madagascar separation from the Afro–Arbian Plate may have caused the shallowing and ultimately the exposure of mid Jurassic carbonate platform forming an erosional unconformity, b) early Cretaceous (Berreiasian) black clays and the interbedded clastics of the Parh Limestone (equivalent to the Sembar Formation) relates to the thermal uplift of the eastern margin of the Indo-Pak Plate and reworking of the late Jurassic paleosoles of the Chiltan Formation in the deep marine settings. c) The constituent facies of the Accretionary Prism Sediments (APS) and its stratigraphic relationship within the study area confirms that its obduction is related to the middle Cretaceous (late Coniacian-early Santonian) around 84-86 Ma during passive margin phase of the Indian Plate d) The uplift of the middle Eocene (Lutetian) carbonate platform is evident from the deposition of the fluvial reddish clays which are sandwiched between the foraminiferal limestone of the Kirthar Formation. The study area has promising reservoir rock potential, with multiple horizons present. Notable candidates include the Chiltan limestone, Parh Limestone, and various dolomite and sandstone horizons. The Ghazij Formation, rich in shale, is an ideal seal. However, an angular unconformity at the base of the Kirthar Formation suggests Eocene deformation, raising uncertainties about its presence. Despite these uncertainties, the study area has favorable geological characteristics for a viable petroleum system.

Keywords: Balochistan Basin; Tectonostratigraphic evolution; Kithar Range; Biostratigraphic and facies augmented information; Petroleum system

1. Introduction

The Kalat and Mach area of the northern Kirthar Range lies in the Balochistan Basin (Neotethys remnant) along the Indus Suture (Axial Belt) evolved due to the oblique collision of the Indo-Pakistan subcontinent with the Afghan and Eurasian Plates, which is part of the Gondwana fragment (Bannert et al., 1992).

There are two major structural elements, namely the Chaman Transform Fault and the Western Indus Suture, which rim the Balochistan Basin towards west and east. The Indus Suture is divided into the Northern Indus Suture and Western Indus

Suture. The Northern Indus Suture (Fig. 1) is located in the northern part of the Indus Basin in north to NW Pakistan, while the Western Indus Suture is located on the western extremity of the Indus Basin along Bela, Khuzdar, Ghazaband, Gawal, Khanozai, Muslimbagh, Zhob, and Waziristan (Fig. 1).

This basin is equated with Central Basin Platform Zone 11 in the regional tectonic framework by Shah and Quindell (1980). The Balochistan Basin represents Triassic to recent (flysch) sedimentary strata with igneous, metamorphic, and mélange rocks. Its complex tectonic setting is characterized by the Cenozoic flysch deposits, an accretionary wedge complex, and a magmatic island arc system. The study area of Kalat and Mach region exhibits a stratigraphic succession ranging from the Jurassic to Sub-Recent sediments, primarily comprising Cretaceous and Jurassic marine deposits that accumulated in a shelf environment under fluctuating marine conditions within the Tethyan Ocean.

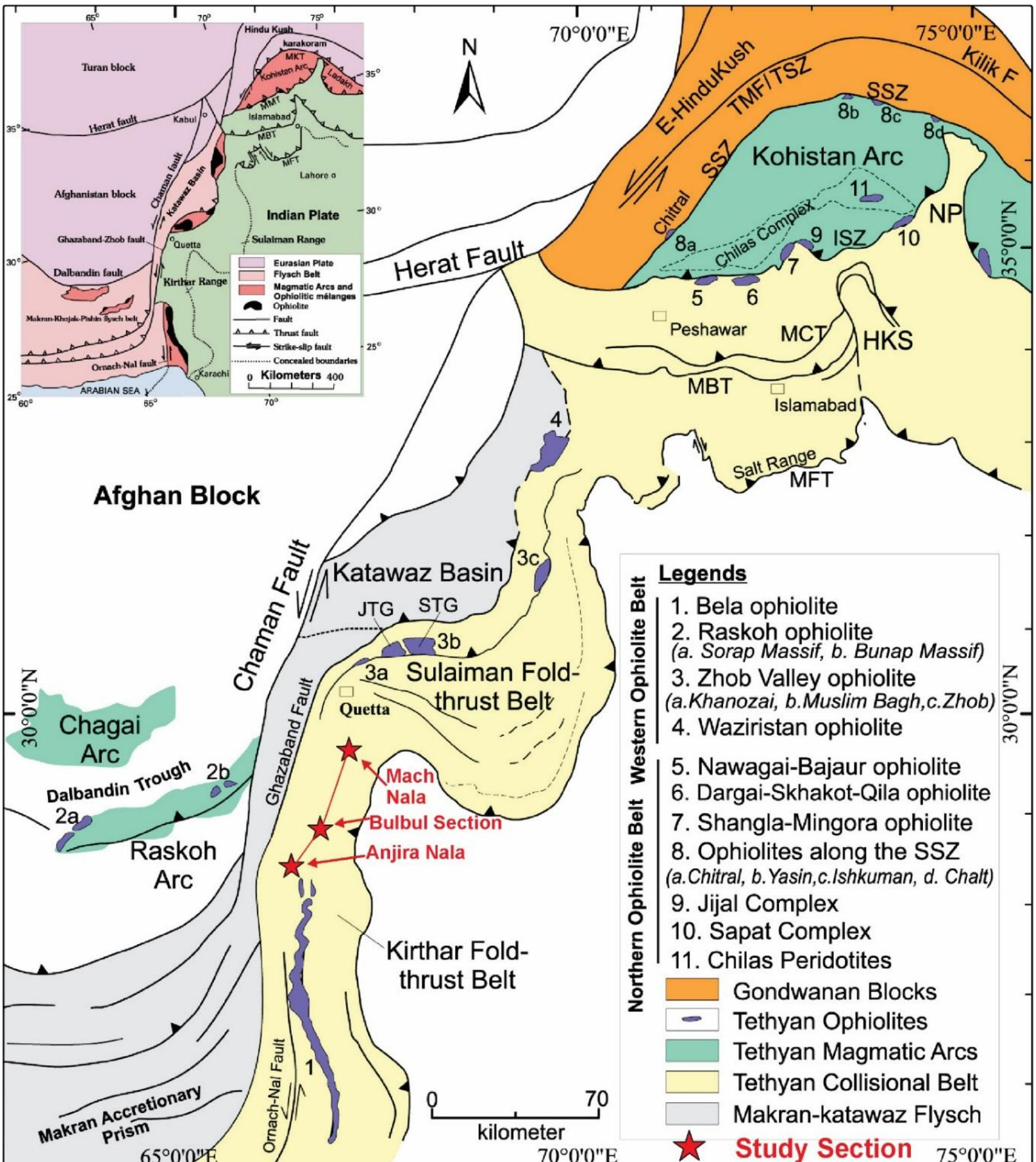

Fig. 1. Generalized tectonic map of Pakistan, inset shows the study after Beck et al. (1996).

The oldest exposed sedimentary unit in the area is the Early to Middle Jurassic Chiltan Formation, consisting predominantly of limestone with minor clastic interbeds, locally associated with a Triassic sequence (Shah, 1980). The Jurassic strata experienced erosion during a tectonic uplift event in the Cretaceous. Subsequently, the Early Cretaceous period was characterized by deposition in a restricted, anoxic marine environment, followed by transgressive–regressive cycles that led to the accumulation of shales, lime muds, and carbonates of the Parh Group. During the Late Paleocene, a relative fall in sea level facilitated the deposition of the Dunghan Formation carbonates (Flügel, 2004). The Eocene period was marked by widespread flooding conditions, resulting in the deposition of the Ghazij Formation shales. In the Oligocene, sediment provenance shifted in the western Kirthar Range due to the collision of the Indian and Eurasian plates, forming small, isolated basins where sedimentation persisted through the Miocene to Quaternary, represented by the Nari and Gaj formations. (Fig. 2).

The study of the tectonostratigraphic evolution in the Kalat and Mach area of the northern Kirthar range offers vital insights into the geological history and hydrocarbon potential of the Balochistan Basin. It elucidates complex tectonic and sedimentary processes from the Jurassic to the Eocene, identifies key reservoir rocks like the Chiltan and Parh Limestones, and provides a broader context for understanding regional tectonics, particularly the obduction of Accretionary Prism Sediments during the middle Cretaceous. Additionally, it aids in responsible resource management by characterizing sedimentological features and identifying the Ghazij Formation as an effective seal. The study also highlights geological hazards, laying a foundation for future research while contributing to hydrocarbon and mineral resource management in the region

2. Methodology

Geological fieldwork conducted in the Kalat, Match region of the northern Kirthar Range involved a comprehensive collection of outcrop samples from four distinct stratigraphic sections. This meticulous sampling process was essential for the subsequent preparation of lithostratigraphic charts, which serve as critical tools for visualizing the distribution and characteristics of various facies. Additionally, petrographic thin sections were prepared in the laboratories of the Department of Geology, University of Peshawar. The Nikon (BX 12) polarizing microscope fitted with the camera was used to accomplish a detailed petrographic and sedimentological study of the sixty (60) rock samples.

The analysis included the examination of petrographic features and their photomicrographs, which provided insights into the fossils, mineral composition, and texture of the rocks. Depositional paleoenvironments were reconstructed based on the observed sedimentological characteristics during fieldwork and interpreted sedimentary facies analysis, and through comparison with additional outcropped data known from the existing literature on time equivalent deposits in Pakistan (Rahim et al., 2022; Fazal et al., 2022; Bilal et al., 2022a, b, 2023; Qamar et al., 2023; Ibrar et al., 2024; Shahzad et al., 2024; Khattak et al., 2024; Khan et al., 2025). This thorough investigation aimed to elucidate the depositional environments and develop a depositional model (Dunham, 1962) for the Jurassic-Paleogene strata, thereby enhancing our understanding of the geological history of the area.

The tectonostratigraphic evolution of the Kalat and Mach regions is another prime focus of this study, as it holds significant implications for petroleum exploration in the area. Analyzing the tectonic and stratigraphic relationships within the rock formations has not only contributed to the academic understanding of the northern Kirthar Range but also provided valuable insights for future hydrocarbon exploration in the region (Siyar et al., 2023).

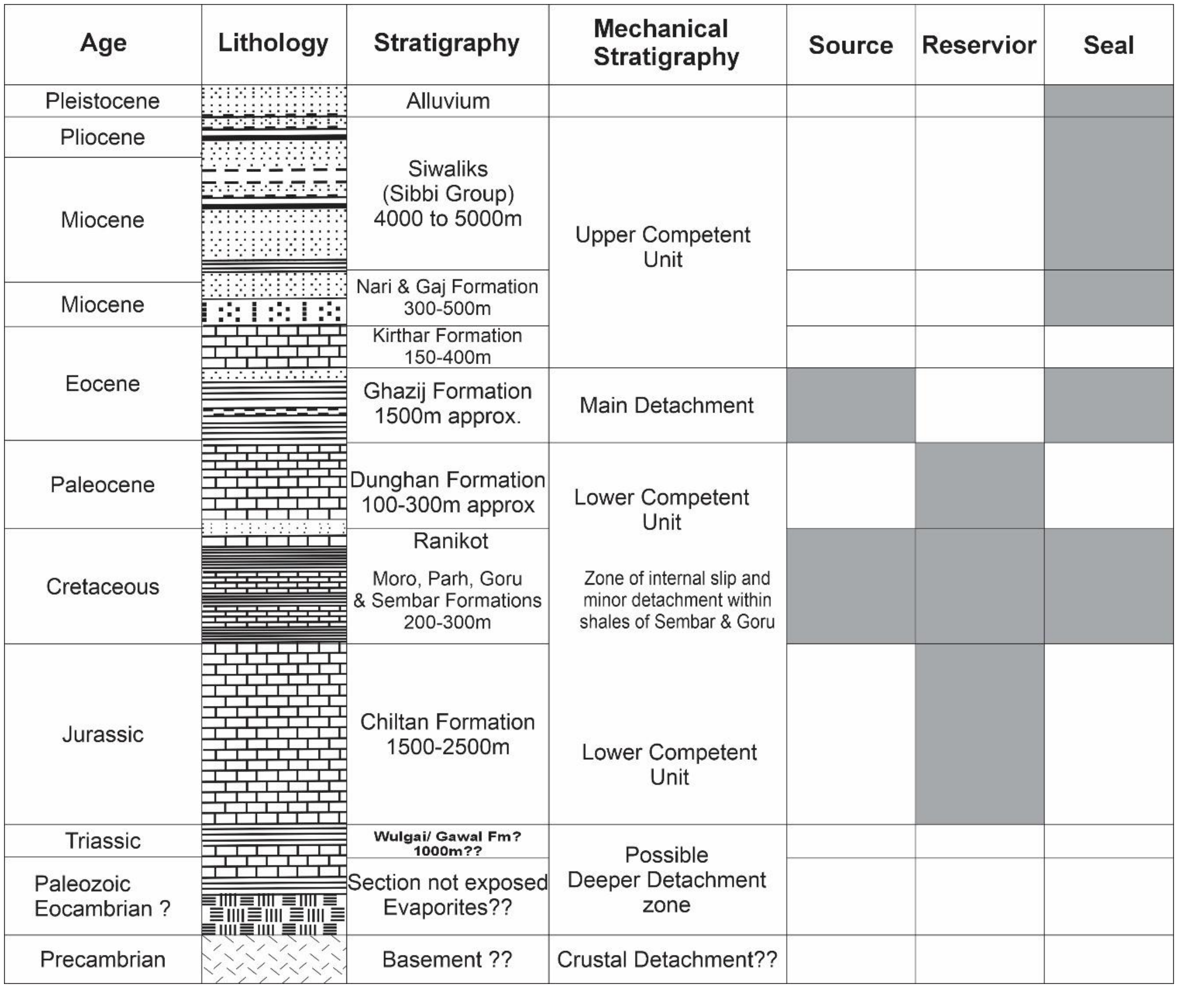

Fig. 2. Generalized stratigraphic column of the study area (Modified after Schelling, 1997, and Maldonado et al., 2011).

3. Result and discussion

3.1. Stratigraphy

The diverse stratigraphy of Pakistan is primarily a consequence of tectonic activities stemming from the collision between the Indian and Eurasian Plates, a process that has been ongoing since the Cretaceous period. The area under investigation showcases a stratigraphic sequence that spans from the Jurassic to the sub-recent, predominantly featuring marine sediments from the Cretaceous and Jurassic periods that were deposited in a shelf environment characterized by varying marine conditions.

The oldest sedimentary unit exposed in the northern to western Kirthar Range consists of early to middle Jurassic limestone, accompanied by minor clastic sediments that are part of an undivided Triassic sequence. During the Cretaceous, the Jurassic stratigraphy experienced significant erosion due to tectonic uplift (Flügel, 2004). The early Cretaceous period was marked by a restricted marine, anoxic environment, which was subsequently followed by transgressive-regressive cycles in the ocean, leading to the deposition of shales, lime mud, and carbonates associated with the Parh group, including the Sembar, Goru, Parh, Pab, Moro, and Ranikot Formations, extending into the early Paleocene. A notable drop in sea level during the late Paleocene facilitated the formation of Dunghan carbonates.

The Eocene epoch saw the deposition of shales from the Ghazij Formation, which occurred under flooding conditions, particularly in the Kalat region, where a substantial thickness of Eocene shales is present along the eastern flank. In the

Oligocene, sedimentation sources shifted in the western Kirthar Range due to the oblique collision of the Indian Plate with the Eurasian Plate and the Afghan Block, resulting in the formation of small, isolated basins where sedimentation persisted until the Quaternary period, with Oligocene and Miocene sediments identified as the Nari, Gaj, and Dada formations. This study aims to establish a new stratigraphic framework and to identify previously unknown stratigraphic units to enhance geological understanding.

Key stratigraphic sections in the Mach nala and Kalat areas have been selected for measuring stratigraphic thicknesses and facies variations, as illustrated in Plates 1 and 2. The following sections provide a detailed description of the studied areas. Stratigraphic sections: Three (03) key stratigraphic sections, namely Mach Nala, Bulbul, and Anjira of Kalat region (Figs. 3-5) have been studied, various stratigraphic units are identified and measured as follows: -

3.2. Mach Nala Section Stratigraphy

3.2.1 Chiltan Formation

A 305-meter-thick section of limestone is composed of greyish limestone with gash veins and light grey micritic nodular limestone interbedded with carbonaceous black clays (Fig. 3). The formation is rich in gastropods, pelecypods, solitary corals, oysters, algae, intraclasts, planktic foraminifers, brachiopods, and peloids. Petrographic analyses reveal the presence of encrusting algae, intraclasts, planktic foraminifera, brachiopods, and peloids. These components indicate deposition in a shallow subtidal marine environment, characterized by fluctuating energy conditions ranging from low to high energy settings. The Chiltan Formation's age is generally stated as Jurassic, but biostratigraphic analysis of the samples yields an age of middle to late Jurassic. The lower contact of the formation is not exposed in the study area, and its upper contact is disconfirmed with Parh group rocks, which contain the laterite beds (Plate 1, Fig. A).

3.2.2 Parh Group

In Mach Nala of the study area, 510m of the Parh Group rocks are measured (Fig. 3), whereas Shah (1980) reported 268m of its thickness at the type section in the Sulaiman Fold Belt. This Formation contains distinctive limestone, which is light grey to creamy white, wackestone to mudstone with a conchoidal fracture. Planktic foraminifera, nano-fossils, and small benthic foraminifera were identified in the analyzed thin section, indicating a late Cretaceous age. The formation has confirmable and disconfirmable contact with overlaying Dughan and underlying Chiltan Formation (Plate 1, Fig. B). Samples from the Parh Group have negligible organic content and present abundant bedding-parallel stylolites in the outcrop. Towards the top, it also contains thinly bedded maroon-colored limestone with carbonaceous shales and greenish splintery clays (Plate 1 Fig. C). The Parh Group was likely deposited below storm wave base in a distal position on an open marine shelf, based on the lack of sedimentary structures, subaerial exposure, and macrofossils.

3.2.3 Dunghan Formation

The Dunghan Formation is measured 90m thick and dominated by black to dark grey, pyritic, intraclastic wackestones with nodular and wavy bedding (Fig. 3). The limestones are thick, coarse-grained grained and horizontally burrowed with Thalassinoides. The formation exhibits well-developed glauconitic peloids and an abundance of reworked benthic foraminifera, bivalves, and algal oncoids. Faunal analysis suggests deposition in a middle to outer neritic environment, characterized by normal marine salinity and low-energy conditions. The occurrence of reworked *Nummulites* within limestone clasts further indicates a Late Paleocene to Early Eocene age for the formation. At Mach Nala, it has confirmable and disconformable contacts with Ghazij shales of Eocene and Cretaceous age Parh group rocks (Plate 1 Fig. D).

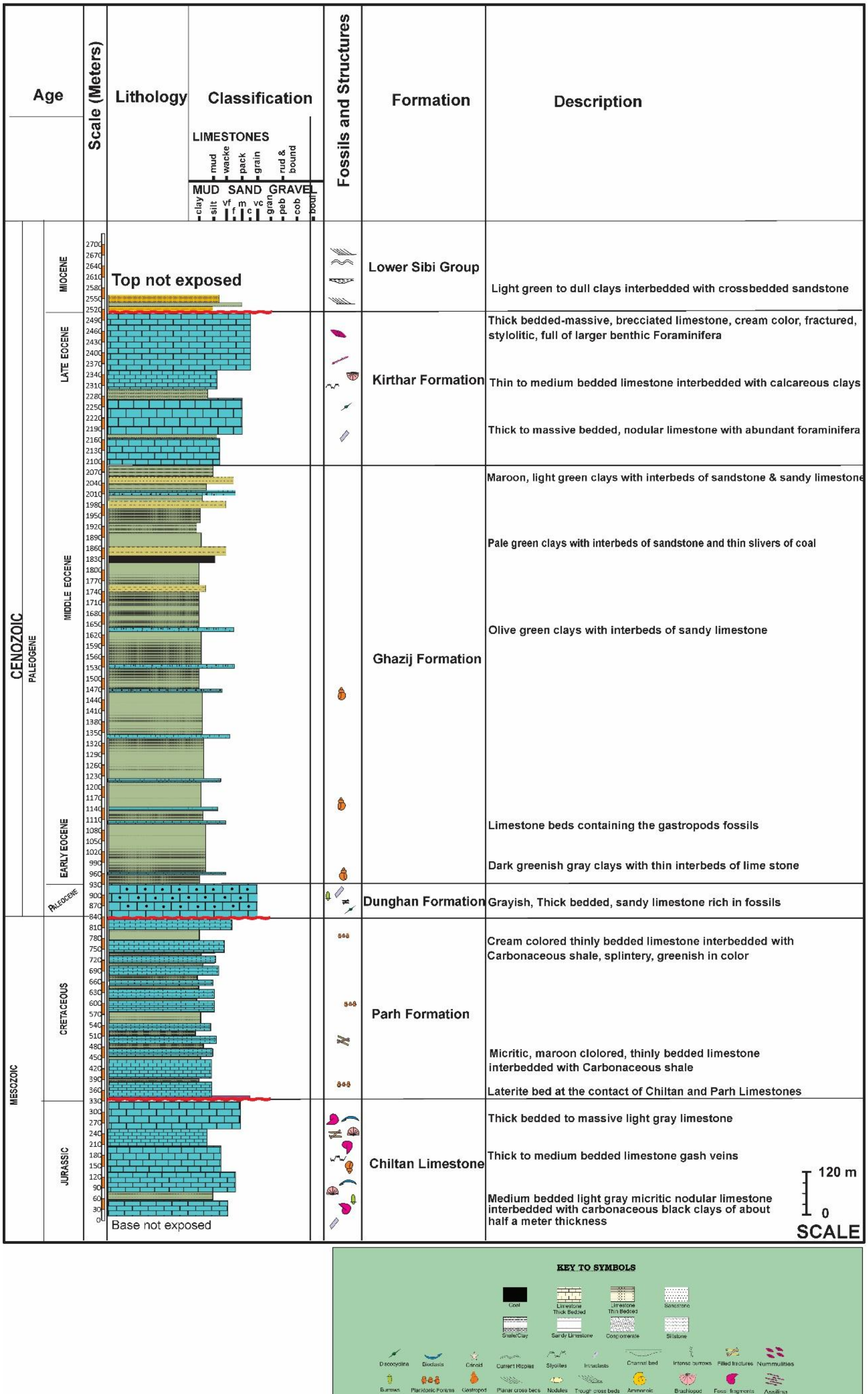

Fig. 3. Composite stratigraphic column of the Mach Nala.

3.2.4 Ghazij Formation

The Ghazij Formation is 1050m thick in the Mach Nala. The Formation contains thick greenish grey to olive green clays with intercalations of sandy limestone beds with coal seams at places (Fig. 3). Biostratigraphy and faunal analyses show an age from early to middle Eocene with a shallow, inner neritic, normal salinity, and high energy conditions (wave- to tide-dominated). Whereas the construction of muddy barrier islands does not indicate a deltaic origin for the Ghazij siliciclastics. The formation has transitional and conformable upper and lower contacts with the Kirthar and Dunghan formations (Plate 1, Fig. E).

3.2.5 Kirthar Formation

The study area measures over 400m thick interbedded limestone with minor clays on top of the Ghazij Formation (Fig. 3). The limestones are abundant with larger benthic foraminifera, and the succession has dominant lithologies including peloid-foraminifera pack/grainstone and peloid-skeletal pack/grainstone. It has lower transitional contact with the Ghazij formation (Eocene) and upper unconfirmable with the Gaj formation of the lower Sibbi group rocks (Miocene) (Plate 1, Fig. F). Faunal analyses on several samples yielded an age of late Eocene.

3.2.6 Lower Sibbi Group

It includes the Gaj, Manchar Formations and belongs to the Siwaliks. In the study area (Mach Nala section), only a 50m section of the Gaj formation is exposed, which contains greenish grey to dull clays with interbedded sandstones (Fig. 3). The sandstones are cross-bedded and relatively thinner to medium-bedded, fine- to coarse-grained grained commonly fining upward with erosive bases. It has unconfirmed lower contact with the Kirthar Formation (Eocene), and the upper contact is not exposed. Duncan and Sladen (1884, 1886), Vredenburg (1909), Nuttall (1925, 1926), HSC (1961), Khan (1968), and Iqbal (1969) reported foraminifers, corals, mollusks, echinoids, algae, and other fossils and assigned an Oligocene to early Miocene age.

3.3 Kalat Region Section Stratigraphy

The rocks of Jurassic-Eocene age are exposed in the Kalat region. Many prominent Ranges and high peaks of (Chiltan, Takatu) are formed by Jurassic rocks. These prominent hills are located in the vicinity of Khuzdar, Karkh, Zahri, Johan, Mazar Drik, Quetta, Ziarat, Kalat, and the Bolan region of the northern Kirthar Range, where they occupy the resistant cores of the anticlines. The Anjira and Bulbul Nala sections in the Kalat region are selected for measurement of the stratigraphic section, facies discrimination and tectonostratigraphic understanding of the region (Figs. 4-5).

3.3.1 Anjira and Chiltan Formations

The Anjira Formation underlies the Chiltan Formation in the Anjira Nala Section, northeastern Kalat area. It is comprised of thinly bedded limestone with minor shale intercalations (Plate 2, Fig. A). The Chiltan Formation comprises a massive, thick-bedded, dark to light grey, light brown limestone and is characterized by variable textures of micrite, ooidal, shelly, and locally pisolithic beds. In the upper part of the Chiltan Limestone. The Formation also contains veins and nodules of chert. Rare fossil fragments of echinoids, pelecypods, brachiopods, and foraminifera are present. It has been assigned a middle Jurassic age (Fatmi, 1977).

3.3.2 Cretaceous Rocks

According to Fatmi (1977), in most regions, the Upper Jurassic and Lower Cretaceous strata are predominantly arenaceous and argillaceous in the lower part, overlain by marine carbonate and clastic sediments in the upper portion of the Lower Cretaceous succession. In the Kohat–Potwar geological province, the Lower Cretaceous is chiefly represented by carbonate lithologies (Ahmad et al., 2022). However, in the Lower Indus Basin, Axial Belt, and Balochistan Basin, the succession comprises shale, marl, limestone, basic lava flows of spilitic composition, radiolarian chert, and other basic to ultrabasic intrusives, which are lithologically comparable to the coloured Mélange described from Iran and Turkey (Shah, 1980; Shah, 2009).

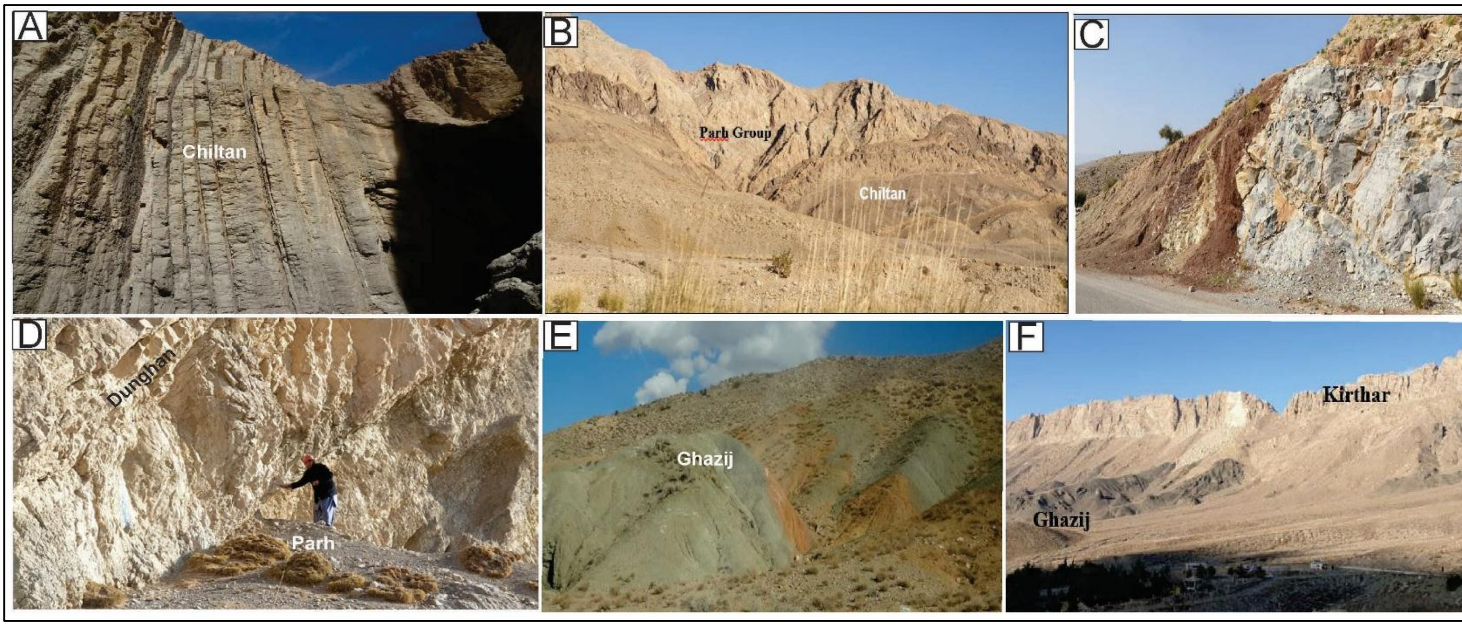

Plate 1

Not to scale

A. Vertical bedded Limestone of Chiltan Formation at Mach Nala Section
B. Outcrop of Chiltan Formation and overlaying Parh Group rock at Mach Nala Section
C. Parh Group rocks with light grey to creamish color and conchoidal fractures at the Mach Nala Section
D. Outcrop of Dunghan Formation in the top of Parh Group rocks at Mach Nala Section (Human can be the scale)
E. Outcrop of Ghazij Formation with greenish grey clays at Mach Nala Section
F. Kirthar Formation on top of Ghazij Formation at Mach Nala Section

Plate 2

Not to scale

A. Anjira Formation, the Anjira Nala Section
B. Outcrop of Parh Limestone in the Bulbul Nala Section
C. Iron crust formed on the Parh Limestone in the Anjira Nala Section
D. Varied colour pelagic clays within the Accretionary Prism sediments
E. Variety of volcanic rocks within the Accretionary Prism sediments (Man can be used as a photo scale)
F. Outcrop of the Ghazij Formation
G. The Karstified surface of the Kirthar Limestone, near Harboi Anticline
H. Outcrop of the Marap Conglomerate near the Harboi Anticline in the Kalat region

3.3.3 Parh Limestone

In the Kalat area, both previous studies and the present investigation document the widespread occurrence of Parh Limestone outcrops (Plate 2, Fig. B). The formation is characterized by hard, light grey to white, cream, and olive-green limestone, which is thin- to medium-bedded, lithographic to porcelaneous, and locally argillaceous, occasionally displaying a platy to slabby texture. Subordinate calcareous shale and marl intercalations are also present. The porcelaneous texture and conchoidal fracture are diagnostic features that distinguish the Parh Limestone from other limestone units in the region. In the lower part, an impersistent maroon-colored limestone bed occurs near the contact with the Goru Formation.

The Parh Limestone is widely distributed across the Axial Belt and Lower Indus Basin. In the type section, it attains a thickness of about 268 m, varying from 300 to 600 m in other localities, and is measured to be approximately 300 m thick in the Bulbul Nala section. The formation is rich in planktonic foraminifera (e.g., *Globotruncana spp*.) and is assigned a Late Cretaceous age. Based on chronostratigraphic correlation, the Parh Limestone is equivalent to the Kawagarh Formation of the Kohat–Potwar geological province (Rehman et al., 2023; Khattak et al., 2024; Khan et al., 2025).

3.3.4 Accretionary Prism Sediments (APS)

In the Kalat region undifferentiated Cretaceous Accretionary Prism sediments (APS) are reported from the northwestern and southwestern parts especially in the Anjira Nala Section (Fig. 4). The APS comprises of the reddish/maroon/greenish shale, marl, creamy limestone, basic lava flows of spilitic type, radiolarian chert, and other basic and ultrabasic intrusive (Plate 2, Figs. C-E). The APS lies above the Jurassic-Cretaceous rocks and below the Paleocene rocks. The measured stratigraphic thickness of the APS in the Anjira Nala Section is recorded as more than 1000m thick (Fig. 4).

3.3.5 Ghazij Formation

In the Kalat area, the Ghazij Formation is recorded as having a more than 500m thick sequence of shale with subordinate claystone and sandstone (Plate 2, Fig. F). In the lower part, olive, brown, maroon, purple, and yellow shale, and green, grey, or brown sandstone exist in the middle-upper part. The Ghazij Formation is widely developed in the Sulaiman, part of the Kirthar Range, and the Axial Belt. It also extends into North Waziristan. The Ghazij Formation conformably overlies the Dungan Formation, and it is unconformably overlain by the Kirthar Formation, respectively. The age of the Ghazij Group is assigned to the Early Eocene (Shah, 2009).

3.3.6 Kirthar Formation

In the Kalat area the most of the exposed outcrops correspond to 300-600m thick carbonates of the Kirthar Formation (Plate 2, Fig. G). The stratigraphic sections along the Bulbul Nala section have a thick sequence of foraminiferal-rich, ridge forming massive-thick bedded limestone. In the lower part, greenish foraminiferal shoals and reddish fluvial facies are present (Fig. 5). The limestone is light grey, cream, or chalky white, weathering to grey, brown, or cream hues. It occurs as thick-bedded to massive units, locally nodular, and occasionally contains algal and coralline structures. The associated shale is olive, yellow, or grey, calcareous, soft, and earthy in texture. In parts of the Kirthar Range, the upper half of the unit forms prominent cliffs composed of massive, fractured limestone (Shah, 2009). The upper contact of the formation is mostly unconformable with the Nari Formation of Oligocene age.

3.3.7 Marap Conglomerate

The Marap conglomerate comprises a thick conglomerate of polymictic, diamictic nature and presents clasts of variable sizes embedded in the fine matrix. It is also forming ridges at places. Various-sized clasts of the Jurassic, Cretaceous, and Paleocene rocks are found within the conglomerate sequence.

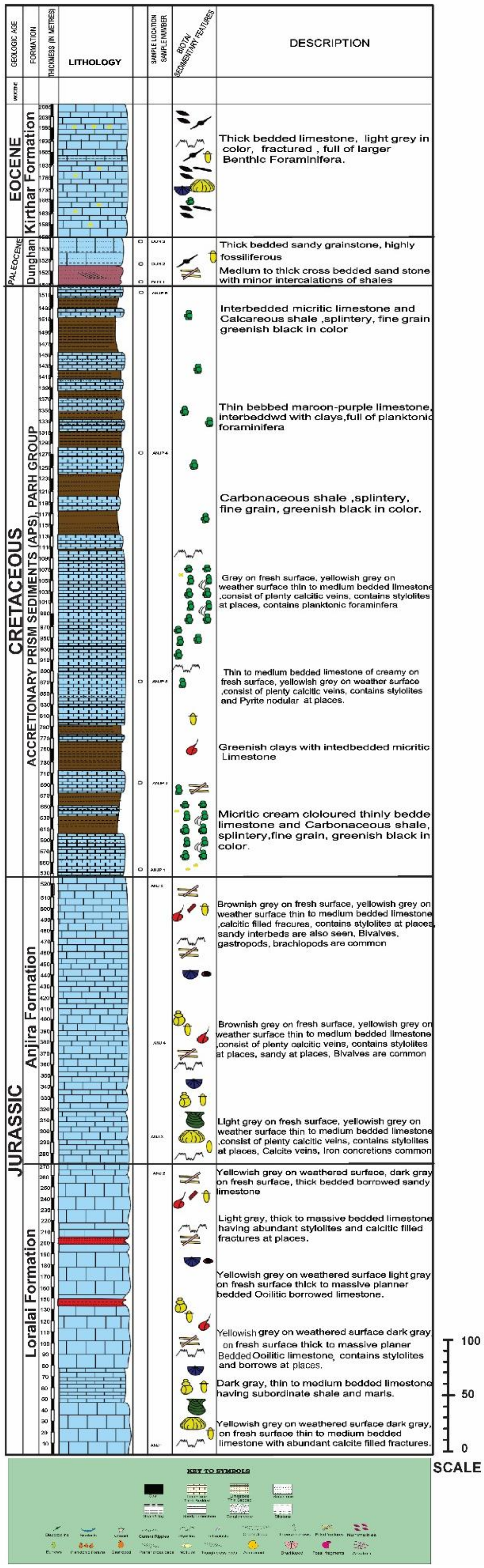

Fig. 4. Composite stratigraphic column of the Anjira Nala.

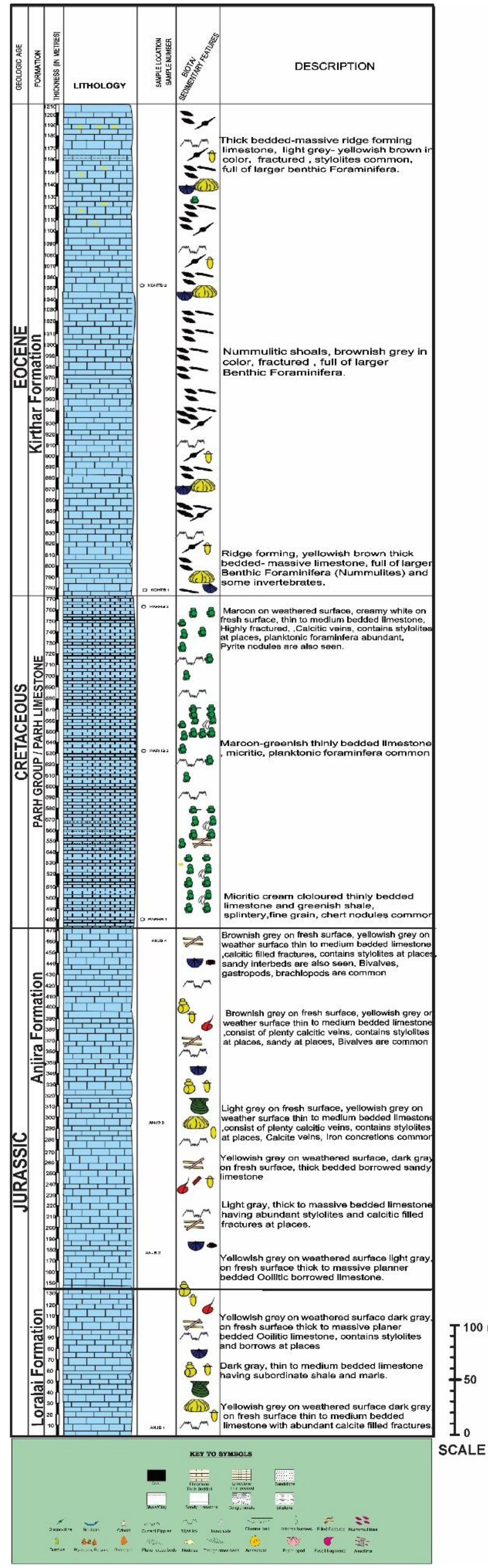

Fig. 5. Composite stratigraphic column of the Bulbul Nala section.

Table 1: The petrographic distribution of various allochems, cements, and other constituents within the Microfacies of the Chiltan Formation in the study area using Dunham (1962) classification.

FORMATION	MICROFACIES	ALLOCHEMS (%)						
		Ooids (%)	Pisoids (%)	Intraclasts (%)	Peloids (%)	Bioclasts (%)	Micrite (%)	Sparite (%)
Chiltan	MCF-I: Ooidal Grainstone Microfacies	50	05	05	10	1-4	Not found	26
	MCF-II: Intraclastic Grainstone	3-5	Not found	25-33	8-10	Not found	Not found	50
	MCF-III: Peloidal Grainstone Microfacies	3-15		5-8	25-70	3-10	10-20	Not found
	MCF-IV: Diverse Bioclastic Grainstone Microfacies	1	2	2	1	63	Not found	32
	MCF-V: Lime Mudstone Microfacies	2	2	Not found	1		82	13

4 Sedimentary Facies and Depositional Model

In the study area, rocks from the Jurassic to Eocene periods are prominently exposed, revealing significant sedimentological characteristics with the following facies:

4.1 Chiltan (Sulaiman) Limestone

In particular, the Chiltan (Sulaiman) Limestone has been analyzed through petrographic studies, leading to the identification of several distinct microfacies. These include the Ooidal Grainstone Microfacies, Intraclastic Grainstone Microfacies, Peloidal Grainstone Microfacies, Diverse Bioclastic Grainstone Microfacies, and Lime Mudstone Microfacies, each one contributing to the overall understanding of the geological framework in this area.

4.1.1 MCF-I: Ooidal Grainstone Microfacies

The Ooidal Grainstone Microfacies is characterized in the field by its massive limestone structure, which can vary from thin to thick bedding and features caves and calcite veins along the bedding planes. Thin section analysis reveals that this microfacies is predominantly composed of ooids, which make up approximately 50% of the constituents, alongside intraclasts (5%), pisoids (5%), peloids (10%), and rare benthic foraminifera (1-3%) (Plate 3, Fig. A/Table 1). These components are embedded in coarse sparry calcite cement, accounting for 26% of the composition. The ooids typically range from 0.15 to 1 mm in diameter and exhibit various microfabrics, including radial-fibrous and concentric structures, while larger ooids over 2 mm are classified as pisoids. The nuclei of the pisoids are generally rounded-oval, formed through the accretion of concentric laminae, which may include bioclasts, ooids, and peloids. Additionally, peloids, measuring 0.05 to 0.1 mm, are rounded and homogeneous, with some rare spherical pellets suggesting a fecal origin. The allochems are moderately sorted, and this sub-microfacies corresponds to Wilson's (1975) Standard Microfacies (SMF). Its diagnostic features include the dominance of ooids as allochems and the presence of coarse sparry calcite cement. The high abundance of ooids, together with the absence of micritic matrix, indicates deposition in a high-energy environment where waves and currents actively reworked and transported carbonate grains. The well-rounded nature of ooids, resulting from concentric laminae enveloping irregular nuclei, further supports this interpretation. Hence, this microfacies is interpreted to have formed in a high-energy, wave-dominated setting, most likely within ooid sand shoals of the inner shelf.

4.1.2 MCF-II: Intraclastic Grainstone

MCF-II: Intraclastic Grainstone Microfacies Field observations reveal that the Intraclastic Grainstone Microfacies is characterized by dark gray, thickly bedded to massive limestone interspersed with thinly laminated shale layers. Thin section analysis shows that this microfacies contains a significant proportion of intraclasts, ranging from 25% to 33% (Table 1), with individual intraclast diameters typically between 4 and 5 mm, and it is differentiated based on its irregular shape from the peliods. The composition is heterogeneous, featuring poorly sorted intraclasts alongside bioclastic fragments, peloids, micrite, and ooids. Additional components include ooids (3-5%), peloids (8-10%), with coarse sparry calcite cement constituting over 50% of the material (Plate 3, Fig. B). This microfacies aligns with SMF 15 of Wilson's SMF model (1975). The presence of poorly sorted intraclasts and sparry cement suggests that this microfacies formed in a storm-dominated inner shelf environment.

4.1.3 MCF-III: Peloidal Grainstone Microfacies

The Peloidal Grainstone Microfacies is characterized in the field by its dark grey appearance on fresh surfaces, which weathers to a lighter grey. This limestone exhibits varying bedding thickness, from thin to thick, and contains calcite-filled veins. Under thin section analysis, the microfacies predominantly consists of peloids, comprising 25-70% of the composition, alongside minor constituents such as intraclasts (5-8%), ooids (3-15%), and bioclasts (3-10%), all embedded within a micrite matrix (Plate 3, Fig. C-D, Table 1). The peloids are generally oblate to rounded, moderately to well sorted, and range in size from 0.003 mm to 0.02 mm, suggesting a fecal origin. The bioclasts include echinoderms, small foraminifera, miliolids, brachiopods, and various undifferentiated fragments. The allochems are arranged in a loosely to closely packed manner, with grain contacts varying from floating to pointed, aligning with SMF 18 of Wilson's SMF model (1975). The interpretation of this microfacies suggests that its mud-free nature, along with the moderate to well-sorted grains and spar cement, indicates deposition under high-energy conditions. However, the presence of peloids, typically associated with low-energy environments, reflects a textural inversion within this high-energy setting.

4.1.4 MCF-IV: Diverse Bioclastic Grainstone Microfacies

The MCF-IV classification identifies a distinct Ooidal Grainstone Microfacies characterized by a gray, dense, and compact with diverse fauna. In terms of composition, bioclasts constitute 63% of this microfacies, while cement accounts for 32%, and other allochems make up the remaining 5% (Table 1). The bioclasts include various foraminifera types (uniserial, coiled uniserial, miliolid, and biserial), undifferentiated bioclasts, echinoderms (such as crinoids and echinoids), brachiopods, and gastropods, all set within a matrix of sparry cement (Plate 3, Fig. E). Notably, foraminifera and echinoderms are frequently observed, aligning with the characteristics of SMF 18 as described in Wilson's model (1975). The presence of coarse spar cement alongside a rich assemblage of bioclasts, including fragments of foraminifera, echinoderms, gastropods, and brachiopods, indicates that this microfacies was formed in a high-energy, wave-dominated shallow shelf environment.

4.1.5 MCF-V: Lime Mudstone Microfacies

The Lime Mudstone Microfacies, observed in the field, consists of thick-bedded to massive limestone layers interspersed with dark grey shales at the base. Thin section analysis reveals that the microfacies is primarily made up of lime mud, which constitutes up to 82 % of the matrix, with trace amounts of allochems, around 5 %, primarily in the form of bioclasts such as echinoid spines and bivalves (Plate 3, Fig. F; Table 1). The remaining 13-15 % consists of micropars formed during diagenesis, aligning with the characteristics of SMF 3 in Wilson's Model (1975). This microfacies is indicative of a depositional environment situated below the storm wave base or within a restricted shelf setting, characterized by a predominance of lime mud and limited biological activity.

4.2 Parh Limestone

4.2.1 Planktonic Foraminiferal Wackestone Microfacies

The microfacies of the Parh Limestone or Parh Group, specifically identified as "Planktonic Foraminiferal Wackestone Microfacies," have been characterized through detailed petrographic analysis. In the field, this microfacies is recognized by its thin to medium bedding and dark gray coloration, which is enriched in planktonic foraminifera. Thin section examinations reveal that this microfacies comprises approximately 25-40% planktonic foraminifera, alongside a minor presence of small benthic foraminifera (around 2%), all set within a lime mud matrix that constitutes 60-75% of the composition (Table 2). The planktonic foraminifera, including genera such as *Globigerina, Globotruncana, and Globorotalia*, are evenly distributed throughout the matrix (Plate 3, Fig. G-H). Additionally, pyrite is noted as a secondary mineral formed during diagenesis under reducing conditions. When compared to Wilson (1975) SMF model, this microfacies aligns closely with the characteristics of SMF 3. The predominance of lime mud and the presence of planktonic foraminifera suggest a depositional environment characterized by low energy, typical of an outer shelf setting.

4.3 Dungan Formation

The Dungan Formation exhibits distinct lithofacies as revealed through petrographic analysis, specifically categorized into two primary types: DFL-I, which is identified as Quartzarenite Lithofacies, and DFL-II, recognized as Calcareous Quartzarenite/Sandy Limestone Lithofacies.

4.3.1 DFL-I: Quartzarenite Lithofacies

The Quartzarenite Lithofacies, designated as DFL-I, is prominently observed in the Mach Section, where it manifests as light gray, thick-bedded calcareous sandstone. Microscopic examination of this lithofacies reveals a composition predominantly consisting of monocrystalline quartz, exceeding 90 percent, with the absence of polycrystalline quartz (Plate 3, Fig. I; Table 3). The quartz grains are characterized by their subangular to subrounded shapes, exhibiting fine to medium grain sizes. Notably, these grains display uniform extinction, with occasional instances of wavy extinction, and overgrowth textures are also present. According to Pettijohn's sandstone classification from 1987, this lithofacies is aptly classified as "Quartzarenite." In terms of texture, the rock unit is primarily fine-grained, although medium-grained specimens are also noted. The grains demonstrate a remarkable uniformity in size, indicative of well-sorted characteristics. Furthermore, the grains exhibit subangularity and high sphericity, while the cementing material is identified as ferruginous calcite coating. The packing of the grains reveals a cubic to rhombic symmetry, with diffused and concavo-convex contacts between grains, suggesting a close to tight packing arrangement.

4.3.2 DFL-II: Calcareous Quartzarenite/Sandy Limestone Lithofacies

This lithofacies is observed in the field as a light gray, thick to massive bedded sandy limestone, often referred to as calci turbidites, interspersed with greenish clay partings. Microscopic analysis reveals a diverse framework mineralogy, predominantly featuring detrital grains, with quartz constituting a significant portion, ranging from 50 to 70 % (Plate 3, Figs. J-K; Table 3). The quartz grains are primarily monocrystalline, with rare occurrences of polycrystalline varieties, and are typically coated with phosphorite minerals, resembling superficial ooids. The grain size varies from fine to coarse, with some exceptionally coarse grains also noted, exhibiting subangular to subrounded shapes and displaying uniform extinction characteristics. Additionally, rock fragments are present in trace amounts, comprising medium-grained chert and siltstone, while bioclasts account for up to 10 % of the composition, often coated with authigenic phosphoritic minerals that impart an ooidal appearance due to prevailing conditions in a shallow marine environment. Authigenic minerals include phosphate-coated grains, glauconite serving as cement, and diagenetic products such as pyrite and dolomite. The formation of phosphate is attributed to shifts in physicochemical conditions in shallow environments, primarily precipitating during periods of non-deposition, while glauconite results from upwelling oceanic currents (Flügel, 2004). Pyrite forms under reducing conditions during diagenesis, filling pore spaces. According to Pettijohn's sandstone classification (1987), this lithofacies is categorized as “Quartzarenite sandstone,” characterized by its abundant bioclasts and sparry calcite cement, along with terrigenous clasts, leading to its designation as “Calcareous Quartzarenitic Sandstone or Sandy Limestone.”

The mineralogical maturity of a rock formation is primarily determined by the relative abundance of quartz, feldspar, and lithic fragments. A higher concentration of quartz signifies a state of super maturity, while an increased presence of feldspar suggests the opposite. In this context, both lithofacies under consideration are characterized by significant quartz content, indicating that they are mineralogically mature. Textural maturity, on the other hand, is assessed through various textural parameters, including grain sorting, roundness, and the amount of clay or matrix present. Based on these criteria, both lithofacies also exhibit textural maturity. Overall, the Dungan Formation demonstrates a distinctly mature profile in terms of both textural and mineralogical characteristics.

4.4 Ghazij Formation

The Ghazij Formation, dating back to the Eocene epoch, has been characterized through extensive field observations, revealing distinct lithofacies. Among these, the Green shale facies is notable for its composition of dark, bluish to green clays and shales, which are interspersed with iron concretions of varying sizes that tend to decrease in abundance towards the upper section. This lower facies transitions from limestone wedges associated with the Dungan Formation, which are embedded within the dark shales of the Ghazij Formation. Additionally, several medium to fine-grained sandstone units are present, exhibiting features such as load casts, asymmetric ripples, and localized laminations. These sandstone units are channel-shaped, characterized by erosive bases and rippled surfaces that taper off laterally. The middle section of the formation is characterized by Shale-sandstone facies, a series of units composed of grey to yellowish sandstone. These sandstone layers exhibit a fine to medium grain size and vary in thickness, interspersed with alternating beds of green to bluish-green shale.

4.5 Kirthar Formation

The Kirthar Formation in the study area reveals a single distinct microfacies, which is characterized by unique compositional elements.

4.5.1 Assilina Nummulites Packstone Microfacies

This Microfacies is primarily composed of significant allochems, including *Nummulites*, *Assilina*, and a smaller presence of *Discocyclina*. In this microfacies, *Nummulites* account for approximately 34% of the composition, while *Assilina* represents around 20%. Additionally, *Discocyclina* and other bioclasts contribute about 18%, with the micrite matrix making up the remaining 28% (Plate 3, Fig. L; Table 4). The depositional environment of this microfacies is interpreted to be situated in a distal inner to proximal middle shelf setting, a conclusion drawn from the presence of *Nummulites* and *Assilina*, alongside the observed Packstone texture indicative of such marine conditions.

5 Depositional Model

The Chiltan (Sulaiman) Limestone was deposited in an inner shelf environment, transitioning from high-energy, wave- and tide-dominated shoals to low-energy slopes beneath the storm wave base, alongside patch reefs (Ahmad et al., 2019). The presence of ooids, pisoids, and sparry cement suggests wave-agitated, shallow water conditions, while the occurrence of sand shoal or barrier ooidal grainstone facies indicates a platform margin sub-environment that separates open marine from restricted marine areas. The prevalence of intraclasts points to sporadic storm events, and the dominance of micrite, coupled with a scarcity of biotic components, suggests significant water depth below the storm wave base (Plate 4, Fig. A).

Table 2: The petrographic distribution of various allochems, cements and other constituents within the Microfacies of the Parh Limestone in the study area.

FORMATION	MICROFACIES	ALLOCHEMS %			
		Planktonic foraminifera (%)	**Ooids (%)**	**Micrite (%)**	**Sparite (%)**
Parh **Limestone**	MCF-I: Ooidal Grainstone Microfacies	25-30%	1-2	40-50%	20%

Table 3: The petrographic distribution of various minerals and other constituents within the Microfacies of the Dungan Formation in the study area (following the Pettijohn et al., 1987).

Thin Section #	**Quartz %**			**Feldspar %**				**Heavy Mineral %**			**Rock Fragment %**	**Total Grain %**	**Clay cement %**	**Chert/Silica %**	**DUNGAN FORMATION MICOFACIES**
								Micas %	**Tourmaline %**	**Monazite %**					
	Q_m	Q_p	Q_t	F_o	F_{pg}	F_{mi}	F_t								
1-3	90	02	82	-	0.5	0.5	01	02	01	01	-	87	05	01	DFL-I: Quartzarenite Lithofacies
	50-70	1-2												01-10	DFL-II: Calcareous Quartzarenite/Sandy Limestone Lithofacies

Table 4: The petrographic distribution of various allochems, matrix, and other constituents within the Microfacies of the Kirthar Formation exposed in the study area.

FORMATION	MICROFACIES	ALLOCHEMS (%)				
		Benthic foraminifera (%)	**LBF**	**Bioclasts (%)**	**Micrite (%)**	**Sparite (%)**
Kirthar Formation	Assilina Nummulites Packstone Microfacies	Nummulites Assilina Discocyclina	34 20 15	1-2	28	Not found

The depositional model for Parh Limestone is characterized by a complex interplay of environmental factors that influence sedimentation processes in marine settings (Jones, 2014; Shah, 2009). The Planktonic Foraminiferal wackestone

Microfacies typically form in open marine environments where nutrient-rich waters promote the proliferation of planktonic foraminifera (e.g., Kontakiotis et al., 2020; Moforis et al., 2022). These microscopic organisms, primarily composed of calcium carbonate, contribute to the sedimentary matrix as they die and accumulate on the seafloor. The wackestone texture indicates a high proportion of fine-grained carbonate mud, which serves as a backdrop for the foraminiferal tests. The depositional environment is often associated with relatively low-energy conditions, allowing for the gradual accumulation of these sediments. Additionally, variations in water depth, temperature, and salinity can lead to distinct stratigraphic layers within the wackestone, reflecting changes in paleoenvironmental conditions over time. Understanding this model is crucial for reconstructing past marine environments and can provide insights into the geological history of sedimentary basins. (Plate 4, Fig. B).

The Dungan Formation reflects a significant shift in its depositional environment (Ahmad et al., 2020). Key indicators such as the presence of phosphate coatings, a high proportion of clastic grains, a diverse mix of faunal remains, and the occurrence of calcitic cement interspersed with bioclasts suggest that the Dungan Formation was deposited in a tidal-dominated delta to subtidal slope setting. This interpretation highlights the dynamic nature of the depositional processes at play, underscoring the complexity of the environmental conditions that influenced the formation of this rock unit (Plate 4, Fig. C).

The interpretation of Ghazij lithofacies indicates a depositional environment marked by low marine energy conditions, with the substantial thickness of the shales suggesting a high rate of sediment deposition in pro-delta settings (Haider et al., 2016) (Plate 4, Fig. D). Notably, the sandstone often features erosive bases, indicative of dynamic sedimentary processes, and is marked by the presence of current ripples, cross-bedding, and burrowing organisms. The sedimentary characteristics observed within the Shale-Sandstone Facies imply that these deposits were formed in delta front environments, where sedimentation is influenced by the interplay of riverine and marine processes (Plate 4, Fig. D).

The depositional environment of Kirthar Limestone is based on the *Assilina-nummulites* paleoecology and sedimentary fabric of the microfacies. It is characterized by a complex interplay of ecological and geological factors that shaped its formation during the Paleogene period (Smewing et al., 2002). These foraminiferal organisms thrived in shallow marine settings, often associated with warm, tropical waters that facilitated their growth and reproduction (Bilal et al., 2022a, b, 2023; Shahzad et al., 2024).

The presence of *Assilina-Nummulites* indicates a well-oxygenated environment, typically found on the continental shelf, where sedimentation rates were moderate (Shahzad et al., 2024). The substrate was likely composed of fine to medium-grained sediments, providing a suitable habitat for these benthic foraminifera.

6 Biostratigraphic Constraints

Macrofossils of the Chiltan Formation include ostracods, algae, corals, bryozoans, brachiopods, mollusks, crinoids, and foraminifera. These assemblages indicate deposition within a shallow carbonate platform environment (Shah, 2009). Based on the occurrence of smaller foraminifera, the Chiltan Formation is assigned to the Bajocian–Callovian stages of the Middle Jurassic in the study area. Fossils recovered from the Sembar Formation comprise belemnites, ammonoids, foraminifera, and nannofossils. The formation is considered Neocomian (Early Cretaceous) in age, and its paleoenvironmental setting is interpreted as shallow to open marine.

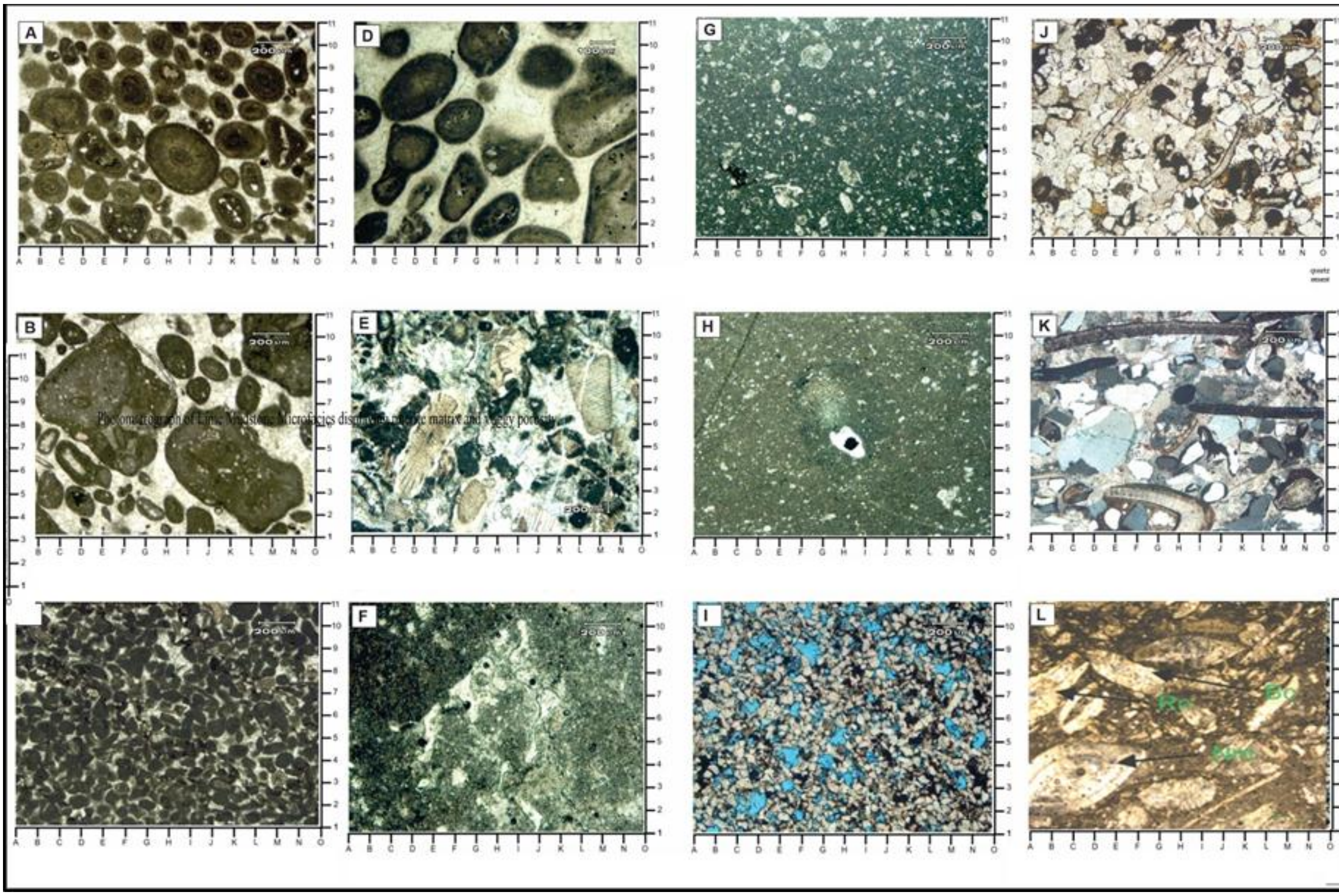

Plate 3

A. Photomicrograph of Ooidal Grainstone Microfacies displaying radial Ooids (I5, BC4) and Peloids (KI 8), embedded in granular spary cement
B. Photomicrograph of Intraclastic Grainstone Microfacies displaying intraclast (E8), ooid (D4), peloid (HI9), Ghost (neomorphism (GI9), embedded in granular mosaic cement
C. Photomicrograph of Peloidal Grainstone Microfacies displaying peloid, embedded in Sparry cement and micro-stylolite with iron oxidation (A05)
D. Photomicrograph of Peloidal Grainstone Microfacies displaying micritized ooids (CD89), peloid (H2), and drusy mosaic cement (HJ78)
E. Photomicrograph of Diverse bioclastic Grainstone Microfacies displaying echinoderms spine and late (Syntacial overgrowth (MN8)) and echinoderms spine longitudinal section (DE5)
F. Photomicrograph of Lime Mudstone Microfacies displaying micrite matrix and vuggy porosity
G. Photomicrograph of Planktonic Foraminiferal Wackstone Microfacies displaying planktonic foraminifera (globigerina (sp.-FG9), globotruncana (sp.-HI4), globorotalia (sp.-EF67) and neomorphism), smaller benthic forams (KL910), embedded in micrite matrix
H. Photomicrograph of Planktonic Foraminiferal Wackstone Microfacies displaying moldic porosity (HI5-pyrite filling) and micrite matrix
I. Photomicrograph of Quartzarenite Lithofacies displaying monocrystalline quartz and intergranular porosity and ferrigenous clay (BC45, H4)
J. Photomicrograph of Quatzarenite Lithofacies displaying monocrystalline quart (H12), Bioclast (neomorphism, DH8), phosphate (HI4, bioclast coating IL4) and clastic cement (GH3)
K. Photomicrograph of Quatzarenite Lithofacies displaying monocrystalline quart (EF7), Polycrystalline quartz (CD4), phosphate coated bioclast (BK10, EH2, MO3)
L. Photomicrograph of the Assilina Bioclastic microfacies showing Nummulites (sp.-Nm), Ranikothalia (sp.-Rn), Assilina (sp.-As), Bioclast (Bc), Micrite (Mic), and Stylolite (Sty)

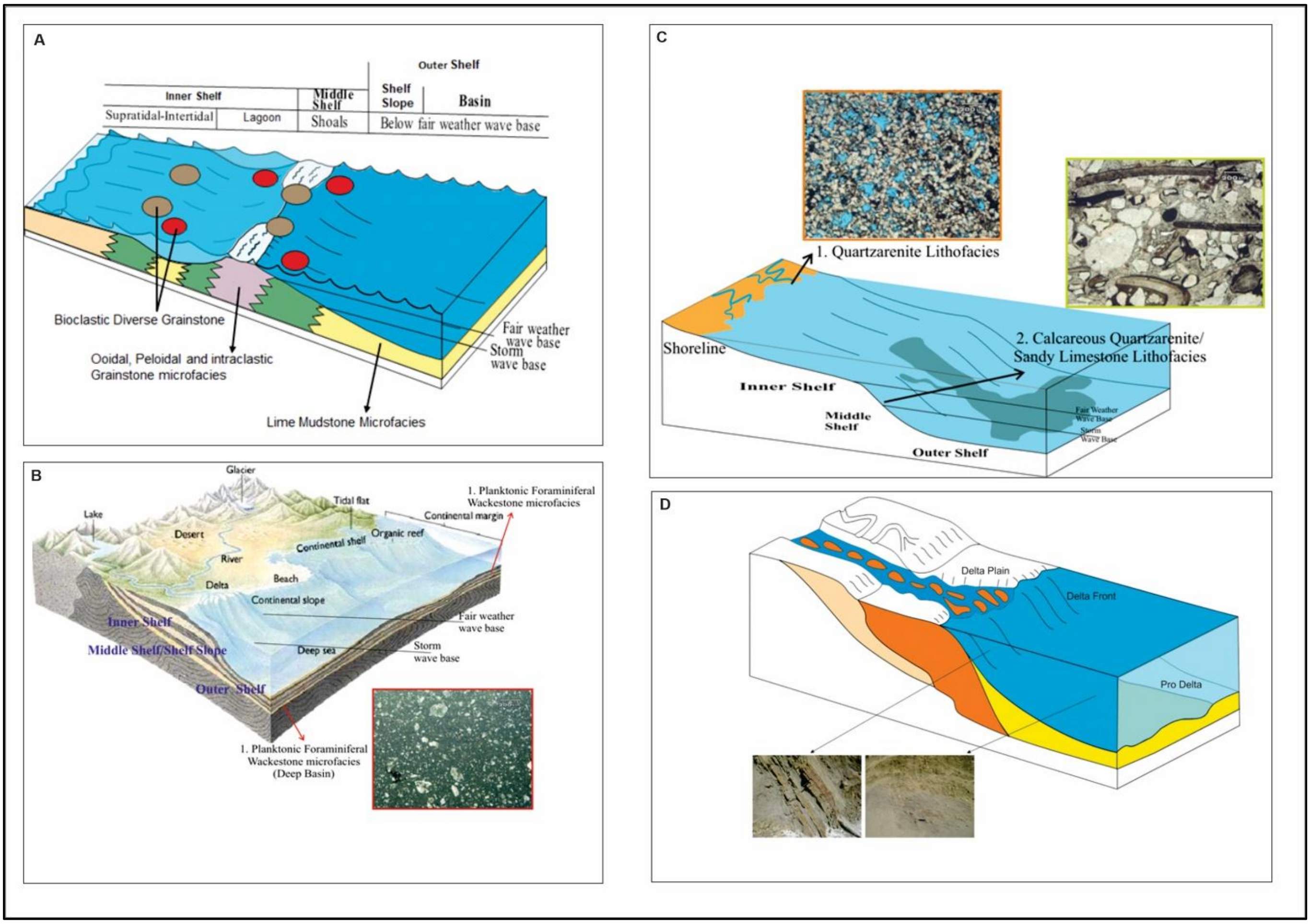

Plate 4

The Plate shows depositional model of the A) Chiltan Formation, B) Parh Formation, C) Dunghan Formation, and D) Ghazij Formation.

The Parh Limestone consists predominantly of limestone, with minor shale and marl interbeds, and is rich in planktic foraminiferal species. Based on its fossil content, the Parh Limestone is assigned a Late Cretaceous age (Shah, 2009). The Paleocene–Eocene succession in the study area mainly comprises carbonates, shales, and sandstones, represented by the Dunghan, Ghazij, and Kirthar formations. The Dunghan Formation is highly fossiliferous, containing larger and planktic foraminifera, red algae, and bryozoans. The larger foraminiferal assemblage—comprising Miscellanea miscella, Lockhartia, Operculina, Discocyclina, Nummulites, and Assilina—suggests a Late Paleocene to Early Eocene age. The Ghazij Formation is dominantly argillaceous, consisting mainly of shale with subordinate limestone, though lithological variations occur locally. The occurrence of smaller benthic foraminifera confirms an Early Eocene age. The record of larger benthic foraminifera (Nummulites *beaumonti*, Assilina *exponense*, etc.) confirms Middle Eocene (Lutetian age)

7 Discussion

7.2 Lateral Facies correlation along the Mach Nala, Anjira nana, and Bulbul Section

The stratigraphic analysis across the three columns, namely Mach Nala, Anjira Nala, and Bulbul Sections (Plate 5), reveals a consistent correlation from the Chilian Limestone at the base to the Lower Siwalik Group at the top, indicating a shift from marine carbonate to fluvial siliciclastic environments. The Chilian Limestone exhibits thick-bedded, fossiliferous limestone, with lateral variations where the Anjira and Bulbul sections show more continuous carbonate with fewer terrigenous interbeds, suggesting a shallow-marine carbonate platform influenced by clastic inputs. In the Parh Formation, the Bulbul and Anjira sections present thicker, cleaner carbonate–marl couplets, while the first column shows a more heterolithic package, indicating increasing clastic influence laterally. The Dungan Formation reveals prominent, distinctive sandstone/sandy limestone packages with bioturbation at Anjira Nala, contrasting with the thicker dark shale–silt in the Mach Nala, reflecting a shift from prodelta to distal delta-front settings. The Ghazij Formation demonstrates numerous sandstone parasequences at Anjira Nala, evidence of storm beds, while Bulbul Nala contains more bioturbated silty mudstone, and the Mach Nala is dominated by shale, indicating an offshore transition. The Kirthar Formation showcases coarsening-upward sand bodies at Anjira, with the Mach Nala being the most distal. The Lower Siwalik Group exhibits a trend toward thicker, grainier fluvial to alluvial deposits at Anjira, suggesting a fluvial depocenter migration. Overall, the analysis illustrates a basinward to landward gradient, with a regressive pattern from marine carbonate to fluvial siliciclastic, punctuated by local transgressive pulses. Practical correlation markers, such as the sharp base contact of the Chilian Limestone and the top flooding shales of the Dungan Formation, further support this synthesis, revealing that the three correlated sections, while recording the same stratigraphy, reflect different lateral facies belts that document a migrating regressive shoreline over time.

7.2 Stratigraphic Evolution

a) Stage 1

Stage 1 of the tectonostratigraphic evolution, during the early Jurassic (Toarcian)-mid Jurassic (Callovian-Alenian) around 180Ma-159.4Ma, is characterized by the deposition of pelagic carbonates from the Anjira Formation, which are found in the Anjira and Bulbul Nala Sections located in the southwestern Kalat region.

This phase in geology is characterized by a series of thinly bedded marine carbonates, which indicate an environment of a deepening basin. The rifting linked to the separation of the Indo-Madagascar landmass from the Afro-Arabian plate is thought to have caused the deepening. During the late Mid Jurassic, the carbonate facies underwent significant shallowing, resulting in the deposition of the Chiltan Formation in the northeastern Kalat region. Evidence of high-energy shallow shelf facies within the Chiltan Formation suggests that the shallow proximal margin of the carbonate platform was actively developing in the northeast, while deeper sedimentation persisted in the southwest, reflecting a dynamic interplay between different depositional environments across the region (Plate 5, Fig. A).

b) Stage 2

During the Late Jurassic period (Kimmeridgian 152-157 Ma), the identification of a karstified surface reaching thicknesses of up to 4 meters, along with paleosols, silcrete, and a ferrecrete horizon extending to 25 meters in the northeastern and northwestern regions of the Kalat region, indicates a significant geological event. This evidence indicates that during the late Mid Jurassic, the platform was fully exposed, resulting in the creation of a sequence boundary. As a result, sediments accumulated during the Late Jurassic. The thermal uplift linked to the detachment of the Indo-Madagascar landmass from the Afro-Arabian Plate is hypothesized to have played a role in the shallowing of the Mid Jurassic Platform, leading to its exposure in the Kalat region (Plate 5, Fig. B).

c) Stage 3 (Plate 5. Figs. B-C)

During the early Cretaceous (Berreiasian), the Sembar Formation's deposition in the northeastern and northwestern regions is closely linked to the redeposition of late Jurassic paleosols from the Chiltan Formation into deep marine environments. The presence of red beds, characterized by a mixture of clays and sandstones within the Accretionary Prism Sediments (APS), can be traced back to this redeposition process, which transported late Jurassic paleosols into deeper basins. This interpretation is further substantiated by the discovery of sedimentary chert nodules embedded within these red beds, which serve as evidence of their deep marine origins. The APS itself is composed of a sedimentary mélange featuring greenish, maroon, and reddish clays interspersed with basaltic volcanic sills, observable in various locations such as the Anjira Nala Section, the Bulbul Road section, and along the Kalat road section. The stratigraphic relationship of the APS within the Kalat region indicates that it has been obducted over the pelagic carbonates of the Parh Limestone and younger sedimentary layers. In the Bulbul Nala Section, the Parh Limestone exhibits a measured stratigraphic thickness of approximately 300 meters, while its association with the APS in other areas of the western Kalat region reveals significant thicknesses exceeding 100 meters. The red beds, which include clays, sands, chert nodules, and planktonic foraminifera, are indicative of the basal fan deposits (above the carbonate compensation depth) of the Sembar Formation, dating from the Valanginian to Barremian stages (approximately 137 to 121 million years ago), Copestake et al. (1996, 1997). These clastic sediments are attributed to the erosion of elevated landforms resulting from thermal uplift during the early Cretaceous (Valanginian) period along the eastern margin of the Indo-Pak Plate (Plate 6, Fig. B).

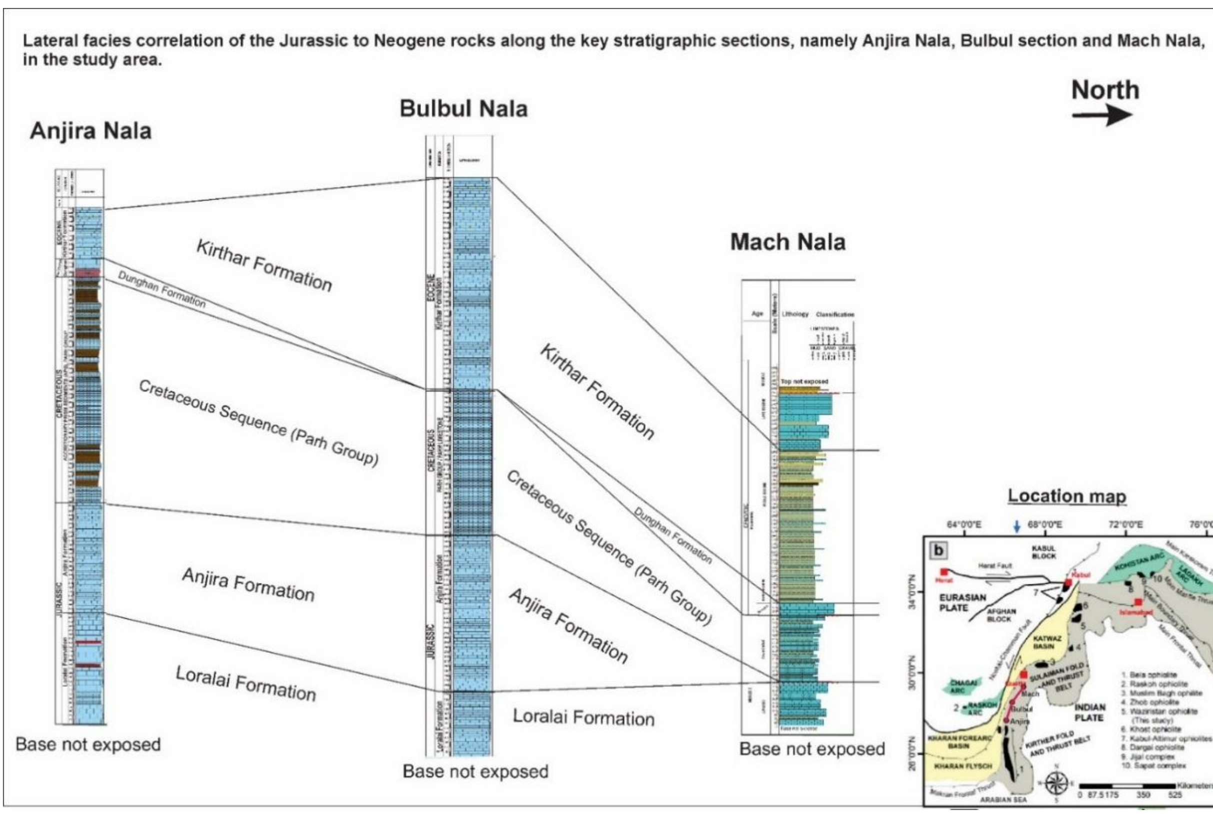

Plate 5: The plate shows lateral facies variation with Jurassic to Eocene rocks of the study area.

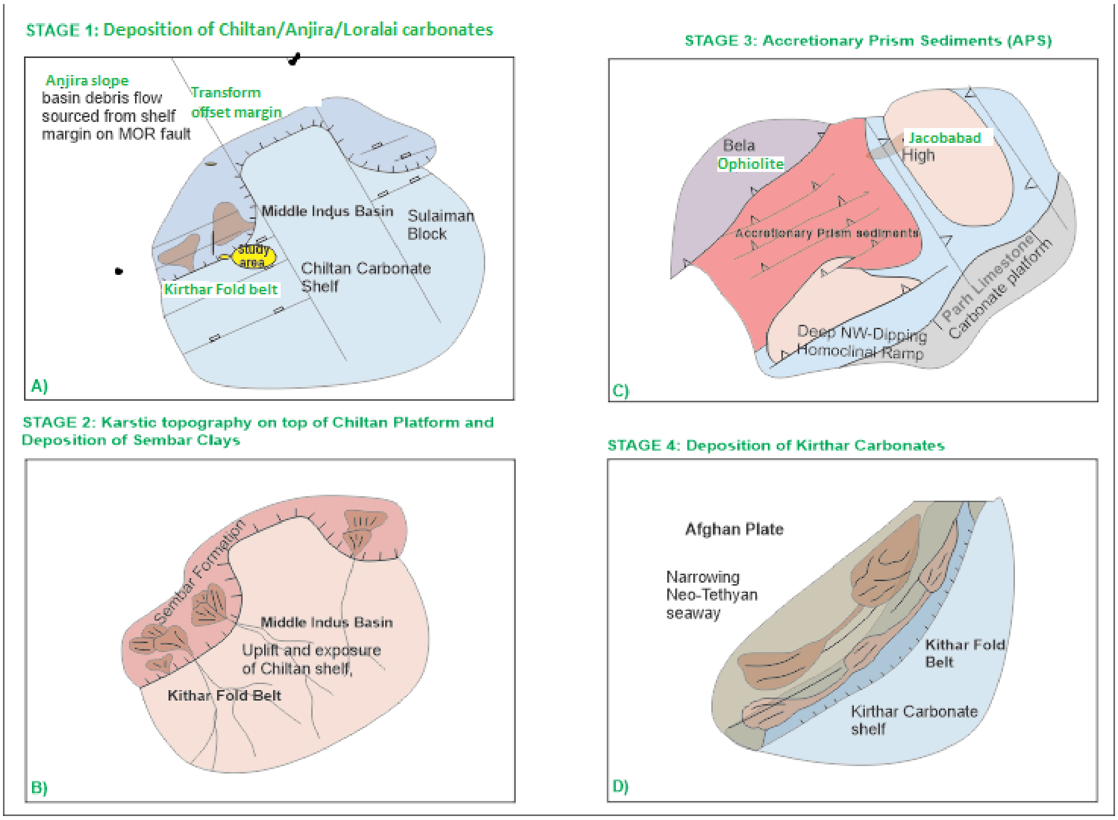

Plate 6: Various stages are shown in the tectono-stratigraphic evolution of the study area.
A) Deposition of the Chiltan/Loralai/Anjira Carbonates during the Middle. Jurassic
B) Karstic topography on top of the Chiltan platform and deposition of Sembar clay's
C) Deposition of Accretionary Prism Sediments (APS)
D) Deposition of Eocene Carbonates (Kirthar)

In the Middle Cretaceous (late Coniacian-early Santonian), around 84-86 Ma, the Parh Limestone, which exhibits a thickness of approximately 300 meters in the Kalat region, shows significant variation across different sections: it reaches 200-300 meters in the southeastern Bulbul Nala Section. This distribution suggests that during the Middle Cretaceous, particularly in the Santonian-Campanian interval, deep basinal conditions prevailed in the southeast, transitioning to shallower environments in the northwest. Furthermore, the timing of the obduction of the Accretionary Prism Sediments (APS) is closely linked to the passive margin phase of the Indian Plate during the late Coniacian to early Santonian period, approximately 84-86 Ma. This correlation aligns with the obduction of ophiolites observed in other regions, such as Waziristan in northern Pakistan, as noted by Beck et al. in 1996. It is possible to explain the lack of late Cretaceous (Maastrichtian) sediments in this context as a result of either non-deposition or erosion of the Fort Munro/Pab sandstone, which aligns with the thermal uplift of the basin that occurred at the same time as the obduction of the Deccan Traps (Plate 6, Fig. C).

In the Anjira Nala section, the Cretaceous-Tertiary unconformity (KT boundary) is evident, showcasing the unconformable contact between the underlying APS and the overlying Dungan Formation, which dates to the Late Paleocene. The presence of the Late Paleocene (Thanetian) transgression's occurrence and extent is substantiated by the Ranikot and Dungan Formations in the Northeastern Kalat region (Smewing et al., 2002). It is worth mentioning that the Ranikot Formation is not present in the southwestern area of Kalat, whereas a 25-meter-thick sandy grainstone facies of the Dungan Formation has been recognized in the Anjira Nala section. This implies that a topographic depression formed in the northeastern area after the deposition of the Ranikot Formation during the Late Paleocene.

d) Stage 4

The early Eocene (Ypresian around 56-47 Ma) sediments of the Laki Limestone are notably absent from the Kalat region; however, the early to middle Eocene (Lutetian) sediments of the Ghazij Formation are found resting uncomfortably atop the Dungan Formation in the north and northeastern regions (Smewing et al., 2002). The shift from the Laki Formation's early Eocene carbonate sediments to the Ghazij Formation's regressive clastic facies coincides with the period when the Indian and Eurasian tectonic plates collided. Moreover, the existence of the Marap Conglomerate positioned above the Ghazij Formation points to a considerable uplift of the basin, impacting rocks that date back to the Jurassic period. This uplift continued until the end of Lower Kirthar carbonate deposition, which has been recorded in most parts of the Kalat region.

The greenish foraminiferal marls and thinly bedded nodular limestone observed represent the transgressive shoals of the Middle Eocene, while the uplift of the Middle Eocene (Lutetian) carbonate platform is further evidenced by the deposition of reddish fluvial clays that are interspersed within the geological record (Plate 6, Fig. D).

7.2 Petroleum System of the Study Area

In the northern Kirthar Range and the Kalat Area, Jurassic strata are predominantly represented by the Chiltan Limestone, which forms the core of most anticlines beneath the Kalat plateau. This limestone also characterizes the anticlinorium zone to the north and northeast of the plateau, where it is prominently featured in the cores of significant geological structures such as Koh-i-Maran, Koh-i-Siah, and Talang. Two notable features of the Chiltan Limestone are its considerable thickness and robust nature, which influence the structural geometries of the major formations. Additionally, the upper section of this unit exhibits extensive karstification and fracturing, often overlain by bauxite and iron oolite deposits found in paleo-topographic depressions (Shah, 2009). Consequently, the Chiltan Limestone not only acts as a reservoir rock but also contributes to the formation of large-amplitude anticlinal structures that are essential for hydrocarbon accumulation. The Cretaceous strata in the study area and its vicinity range from 400 to 800 meters in thickness, encompassing the Sembar, Guru, and Parh formations. The Sembar Formation is noted for its organic richness, indicating its potential as a hydrocarbon source, while various horizons within the upper Cretaceous are recognized for their reservoir capabilities. Furthermore, the relatively incompetent nature of much of the Cretaceous section, particularly the Sembar, Guru, and Parh formations, facilitates structural detachments. The Paleocene section of the study area is represented by the Ranikot and Dungan formations. The Ranikot Formation, composed of limestone, dolomite, and sandstone, presents potential as a reservoir, albeit with a limited thickness of only a few meters. In contrast, the Dungan Formation consists of massive limestone but exhibits significant lateral variations, adding complexity to the geological framework of the area. The hydrocarbon potential of a region is fundamentally influenced by several geological factors, including the presence of one or more stratigraphic horizons that contain source rocks, appropriate reservoir rocks, a stratigraphic unit characterized by low porosity and permeability to act as a seal, and suitable structural formations. In the study area, the Sembar Formation is identified as a potential source rock, although its distribution across the area is notably irregular, raising concerns about the reliability of a suitable source rock in this region. The study area, however, exhibits promising reservoir rock potential, with multiple horizons present within the stratigraphic sequence. Notable reservoir candidates include the karsted and fractured upper contact of the Chiltan limestone, along with its associated bauxite and chamositic ironstone, the dolomitized Parh Limestone, and various dolomite and sandstone horizons within the Upper Cretaceous, as well as the fractured and karsted limestone found in the Palaeocene Dungan Formation. Regarding sealing capabilities, the Ghazij Formation, rich in shale and with a thickness nearing one kilometer, is considered an ideal seal. Nevertheless, the identification of an angular unconformity at the base of the Kirthar Formation indicates that the Ghazij Formation may have been subjected to Eocene deformation, potentially leading to its uplift and erosion before the deposition of the Kirthar Formation. This raises uncertainties about the consistent presence of the Ghazij Formation at subsurface levels throughout the area. Furthermore, the Eocene Kirthar Formation has been observed to directly overlie Cretaceous and, in some locations, Jurassic strata both to the north and south of the Kalat plateau. Despite the uncertainties surrounding the availability of suitable source, reservoir, and seal rocks, the study area possesses several geological characteristics that suggest favorable hydrocarbon prospectivity.

8 Conclusions

This study analyzes stratigraphic and sedimentological data to understand the tectonostratigraphic evolution of the Kalat-Mach region in the northern Kirthar Range, Balochistan Basin, Pakistan.

Four (4) stages of tectonostratigraphic evolution are identified in the area.

- The late early to mid-Jurassic period (approximately 180 Ma to 159.4 Ma) is characterized by the deposition of the Chiltan Formation.
- A late Jurassic thermal uplift, preceding the Indo-Madagascar separation from the Afro-Arabia Plate, likely led to the shallowing and exposure of the mid-Jurassic platform, resulting in an erosional unconformity.
- Early Cretaceous deposition is linked to the re-deposition of late Jurassic paleosols from the Chiltan Formation in deep marine environments.
- Early Cretaceous black clays and the interbedded clastics of the Parh Group (equivalent to the Sembar Formation) relate to the thermal uplift of the eastern margin of the Indo-Pak plate and redeposition of the late Jurassic paleosoles of the Chiltan Formation in the deep marine settings
- The stratigraphic relationship of the Accretionary Prism Sediments (APS) indicates its obduction is connected to the middle Cretaceous passive margin phase of the Indian Plate (late Coniacian to early Santonian, around 84-86 Ma).
- The absence of late Cretaceous (Maastrichtian) sediments may result from non-deposition or erosion in the thermally uplifted basin.
- The Cretaceous-Tertiary unconformity (KT boundary) is represented by Cretaceous APS and the late Paleocene Dunghan Formation.
- The transition from the early Eocene carbonate sediments of the Laki Formation to the regressive clastic facies of the Ghazij Formation corresponds with the early Eocene collision between the Indian and Eurasian plates. Where the evidence of subsequent uplift during the middle Eocene (Lutetian) is indicated by the deposition of fluvial reddish clays over the Kirthar carbonates
- The study area exhibits significant reservoir rock potential, featuring multiple geological horizons such as Chiltan limestone, bauxite, ironstone, Parh Limestone, and various dolomite and sandstone layers. The Ghazij Formation, abundant in shale, serves as an effective seal for potential reservoirs.
- An angular unconformity at the base of the Kirthar Formation indicates Eocene deformation, introducing some uncertainties regarding its geological continuity.

Acknowledgements

We would like to thank the anonymous reviewers for their vigilant evaluation of our initial manuscript and their insightful comments and useful suggestions.

Author's Contribution

Irfan Khan proposed the main concept, conducted fieldwork, sampling, mapping, section measurements, and did data *interpretation, correlation, result, manuscript writing, addressed reviewers' comments, and submissions. 1Sajjad Ahmad assisted in establishing the sedimentological and tectonostratigraphic framework, section measurement, sampling, addressed the reviewers' comments, and thoroughly proofread the manuscript before and after submission. 2Sajjad Ahmad supervised in the fieldwork, mapping, and tectonic history analysis and contributed to the revisions based on reviewers' feedback. Gohar Rehman provided relevant literature, assisted with geological mapping, and Structural modeling. Irfan Fiaz helped in the data collection and petroleum system interpretation, ultimately enhancing the quality and depth of the research findings. Salik Javed assisted in formatting the manuscript, ensuring that all text, figures, and plates adhered to the required standards. Benazir Iqbal helped in the CorelDRAW and GIS-related redrafting of various plates and figures*.

Funding: Not Applicable

Data availability

The datasets used and/or analyzed during the study are available on request from the corresponding author.

DECLARATIONS

Conflict of interest: The authors declare no competing interests.

Ethics approval and consent to participate.

The authors declare that they followed the ethics in scientific research.

Consent for publication.

Not applicable

Competing interests

The authors declare no competing interests.

Conflict of interests: The authors reported no potential conflict of interest.

References

Ahmad, I., Shah, M. M., Janjuhah, H. T., Trave, A., Antonarakou, A., & Kontakiotis, G. (2022). Multiphase diagenetic processes and their impact on reservoir character of the Late Triassic (Rhaetian) Kingriali Formation, Upper Indus Basin, Pakistan. *Minerals, 12*(8), 1049. https://doi.org/10.3390/min12081049

Ahmad, S., Wadood, B., Khan, S., Abdullah, M., Mustafa, G., Hanif, M., & Ullah, H. (2020). The sedimentological and stratigraphical analysis of the Paleocene to Early Eocene Dungan Formation, Kirthar Fold and Thrust Belt, Pakistan: Implications for reservoir potential. *Journal of Sedimentary Environments, 5*(1), 1–14. https://doi.org/10.1007/s43217-020-00027-2.

Ahmed, A., et al. (2019). Paleobiodiversity and tectono-sedimentary records in the Mediterranean Tethys and related eastern areas (pp. 167–170). In M. Boughdiri, B. Bádenas, P. Selden, E. Jaillard, P. Bengtson, & B. R. C. Granier (Eds.), *Paleobiodiversity and tectono-sedimentary records in the Mediterranean Tethys and related eastern areas* (Advances in Science, Technology & Innovation, pp. 167–170). Springer. https://doi.org/10.1007/978-3-030-01452-0_75

Bannert, D., Cheema, A., Ahmed, A., & Schaefer, U. (1992). The structural development of the western fold belt, Pakistan. *Geologisches Jahrbuch Reihe B Regionale Geologie Austland*, *80*, 3-60.

Beck, R. A., Sercombe, W. J., & Burbank, D. W. (1996). Late Cretaceous ophiolite obduction and Paleocene India–Asia collision in the westernmost Himalaya. *Geodinamica Acta*, *9*(2), 114–144.

Bilal, A., Mughal, M. S., Janjuhah, H. T., Ali, J., Niaz, A., Kontakiotis, G., Antonarakou, A., Usman, M., Hussain, S. A., & Yang, R. (2022b). Petrography and provenance of the Sub-Himalayan Kuldana Formation: Implications for tectonic setting and palaeoclimatic conditions. *Minerals, 12*(6), 794. https://doi.org/10.3390/min12060794

Bilal, A., Yang, R., Janjuhah, H. T., Mughal, M. S., Li, Y., Kontakiotis, G., & Lenhardt, N. (2023). Microfacies analysis of the Palaeocene Lockhart Limestone on the eastern margin of the Upper Indus Basin (Pakistan): Implications for depositional environment and reservoir characteristics. *The Depositional Record*, *9*(2), 152–173. https://doi.org/10.1002/dep2.223

Bilal, A., Yang, R., Mughal, M. S., Janjuhah, H. T., Zaheer, M., & Kontakiotis, G. (2022a). Sedimentology and diagenesis of the Early–Middle Eocene carbonate deposits of the Ceno-Tethys Ocean. *Journal of Marine Science and Engineering, 10*(11), 1794. https://doi.org/10.3390/jmse10111794

Duncan, P. M., & Sladen, W. P. (1884–1886). Tertiary and Upper Cretaceous fossils of western Sind: Fasc. 2, The fossil Echinoidea from Ranikot series of Nummulitic strata in western Sind. *Memoirs of the Palaeontologia Indica, 14*(1–3), 25–100.

Dunham, R. J. (1962). Classification of carbonate rocks according to depositional texture. In W. E. Ham (Ed.), *Classification of carbonate rocks* (Vol. 1, pp. 62–121). American Association of Petroleum Geologists (AAPG) Memoir.

Fatmi, A. N. (1977). Mesozoic. In S. M. I. Shah (Ed.), *Stratigraphy of Pakistan* (Vol. 12, pp. 29–56). Geological Survey of Pakistan.

Fazal, A. G., Umar, M., Shah, F., Miraj, M. A. F., Janjuhah, H. T., Kontakiotis, G., & Jan, A. K. (2022). Geochemical analysis of Cretaceous shales from the Hazara Basin, Pakistan: Provenance signatures and paleo-weathering conditions. *Journal of Marine Science and Engineering, 10*(6), 800. https://doi.org/10.3390/jmse10060800

Flügel, E. (2004). *Microfacies of carbonate rocks: Analysis, interpretation, and application* (2nd ed., 976 pp.). Springer-Verlag.

Haider, R., Ali, Z. A., & Arif, J. (2016). 3-D facies modeling of Ghazij Formation of the Central Indus Monocline, Pakistan. *[Unpublished report or conference paper]*.

Hunting Survey Corporation. (1961). *Reconnaissance geology of part of West Pakistan* (Colombo Plan Cooperative Project). Toronto, Canada.

Ibrar, M., Khan, S., Rashid, M. U., et al. (2024). Integrated sedimentary and diagenetic constraints for delineating the reservoir potential of Jurassic carbonate sequences in the autochthonous Samana Suk Formation, Attock–Cherat–Nizampur area, Pakistan. *Carbonates and Evaporites, 39*, 51. https://doi.org/10.1007/s13146-024-00951-1

Iqbal, M. W. A. (1969). *The Tertiary pelecypod and gastropod fauna from Drug, Zinda Pir, Vidor (D.G. Khan District), Jhalar and Charrat (Campbellpur District), West Pakistan.* Geological Survey of Pakistan, *Memoir, Palaeontologica Pakistanica, 6*, 77 p.

Jones, R. W. (2014). *Foraminifera and their application.* Cambridge University Press.

Khan, M. A., Rahman, A. U., Kontakiotis, G., et al. (2025). Stratigraphic development and sedimentary characteristics of Upper Cretaceous Kawagarh Formation at Garhi Habibullah section of Hazara Basin, Pakistan. *Carbonates and Evaporites, 40*, 49. https://doi.org/10.1007/s13146-025-01049-3

Khan, M. H. (1968). The dating and correlation of the Nari and Gaj formations. *Geological Bulletin, University of the Punjab, 7*, 57–65.

Khattak, S. A., Hanif, M., Ahmad, S., et al. (2024). Sedimentology and reservoir characterization of Upper Cretaceous Kawagarh Formation, Upper Indus Basin, Lesser Himalayas, Pakistan: Inferences from petrography, SEM–EDS, and petrophysics. *Carbonates and Evaporites, 39*, 72. https://doi.org/10.1007/s13146-024-00972-w

Kontakiotis, G., Moforis, L., Karakitsios, V., & Antonarakou, A. (2020). Sedimentary facies analysis, reservoir characteristics, and paleogeographic significance of the Early Jurassic to Eocene carbonates in Epirus (Ionian Zone, Western Greece). *Journal of Marine Science and Engineering, 8*(9), 706. https://doi.org/10.3390/jmse8090706

Maldonado, F., Mengal, J. M., Khan, S. H., & Warwick, P. D. (2011). Summary of the stratigraphy and structural elements related to plate convergence of the Quetta–Muslim Bagh–Sibi region, Balochistan, west-central Pakistan. *U.S. Geological Survey Open-File Report 1224*, 1–22.

Moforis, L., Kontakiotis, G., Janjuhah, H. T., Zambetakis-Lekkas, A., Galanakis, D., Paschos, P., Kanellopoulos, C., Sboras, S., Besiou, E., Karakitsios, V., et al. (2022). Sedimentary and diagenetic controls across the Cretaceous–Paleogene transition: New paleoenvironmental insights of the external Ionian Zone from the pelagic carbonates of the Gardiki section (Epirus, Western Greece). *Journal of Marine Science and Engineering, 10*(12), 1948. https://doi.org/10.3390/jmse10121948

Nuttall, W. L. F. (1925). The stratigraphy of the Laki series (Lower Eocene) of part of Sind and Balochistan, with a description of larger foraminifera contained in those beds. *Geological Society of London Quarterly Journal, 81*, 417–453.

Nuttall, W. L. F. (1926). The zonal distribution of larger foraminifera of the Eocene of Western India. *Geological Magazine, 63*, 495–504.

Pettijohn, F. J., Potter, P. E., & Siever, R. (1987). *Sand and sandstone* (2nd ed.). Springer-Verlag.

Qamar, S., Shah, M. M., Janjuhah, H. T., Kontakiotis, G., Shahzad, A., & Besiou, E. (2023). Sedimentological, diagenetic, and sequence stratigraphic controls on the shallow to marginal marine carbonates of the Middle Jurassic Samana Suk Formation, North Pakistan. *Journal of Marine Science and Engineering, 11*(6), 1230. https://doi.org/10.3390/jmse11061230

Rahim, H.-u., Qamar, S., Shah, M. M., Corbella, M., Martín-Martín, J. D., Janjuhah, H. T., Navarro-Ciurana, D., Lianou, V., & Kontakiotis, G. (2022). Processes associated with multiphase dolomitization and other related diagenetic events in the Jurassic Samana Suk Formation, Himalayan Foreland Basin, NW Pakistan. *Minerals, 12*(12), 1320. https://doi.org/10.3390/min12121320

Rehman, S. U., Munawar, M. J., Shah, M. M., Ahsan, N., Kashif, M., Janjuhah, H. T., Lianou, V., Kontakiotis, G. (2023). Diagenetic evolution of Upper Cretaceous Kawagarh carbonates from Attock–Hazara Fold and Thrust Belt, Pakistan. *Minerals, 13*(9), 1438. https://doi.org/10.3390/min13091438

Schelling, D. (1997). Structural geology of the northern Bolan Block and the Zarghun Anticline, Western Pakistan. *EGI Technical Report 97-5-20970*, Energy & Geoscience Institute, University of Utah.

Shah, S. M. I. (1980). *Stratigraphy and economic geology of the central Salt Range* (Record 52). Geological Survey of Pakistan.

Shah, S. M. I. (2009). *Stratigraphy of Pakistan* (Memoir 22). Geological Survey of Pakistan.

Shah, S. M. I., & Quennell, A. M. (1980). Stratigraphic correlation of Turkey, Iran, and Pakistan. London: Overseas Development Administration.

Shahzad, A., Kontakiotis, G., Adatte, T., Ahmed, K.S., Riaz, M.T., Janjuhah, H.T., Besiou, E. (2024). Multi-Elemental Chemostratigraphy, Sequence Development, Depositional History, and Environmental Importance of Early Eocene Red Beds (Kuldana Formation) in NW Himalayas, Pakistan. *Journal of Earth Science*, *35*(2), 349-375.

Siyar, S. M., Ali, F., Ahmad, S., Kontakiotis, G., Janjuhah, H. T., Jahandad, S., & Naseem, W. (2023). Organic geochemistry of crude oils from the Kohat Basin, Pakistan. *Geosciences*, *13*(7), 199.

Smewing, J. D., Warburton, J., Daley, T., Copestake, P., & Ul-Haq, N. (2002). Sequence stratigraphy of the southern Kirthar fold belt and middle Indus basin, Pakistan. *Geological Society, London, Special Publications, 195*(1), 273-299.

Wilson, J. (1975). *Carbonate facies in geologic history*. Springer-Verlag.

Vredenburg, E. W. (1909). Report on the geology of Sarawan, Jhalawan, Makran, and the state of Lasbela. *Records of the Geological Survey of India, 38*(3), 189–215.